ACS OMEGA

http://pubs.acs.org/journal/acsodf

Article

Synthesis of Biocompatible Nanoporous ZIF-8-Gum Arabic as a New Carrier for the Targeted Delivery of Curcumin

Seyedeh Fatemeh Khalilian, Maryam Tohidi,* and Banafsheh Rastegari

Cite This: *ACS Omega* 2023, 8, 3245−3257

Read Online

ACCESS | Metrics & More | Article Recommendations | Supporting Information

ABSTRACT: The synthesis of biocompatible nanoporous zeolitic imidazolate framework-8 (ZIF-8) was performed in the presence of gum arabic (GA), curcumin (CCM), and folic acid (FA) as a template for the biomineralization process, a natural anticancer component, and a targeting agent, respectively. The synthesis of ZIF-8-GA-CCM-FA was completed in a single step at room temperature in aqueous media with a minimum amount of ethanol at a linker/metal molar ratio of 10. FA was dissolved by the alkaline medium produced by a 2-methyl imidazolium (HmIm) linker without using any toxic organic solvent or additional conjugation agents. The FA-modified carrier can target the folate receptors on Hela cells. To the best of our knowledge, this is the first report about the one-pot encapsulation of CCM and FA in a biocompatible ZIF-8-GA framework in a green solvent. This method enables high CCM loading in the ZIF-8-GA framework structure (ca. 90%) at a short time of 15 min. The effect of CCM concentration was investigated on the size, morphology, and crystallinity of the synthesized structures. The products were characterized with field emission scanning electron microscopy, Brunauer−Emmett−Teller surface area analysis, X-ray diffraction, Fourier transform infrared, and UV−vis spectroscopy techniques. The release rate of CCM from ZIF-8-GA-CCM-FA was studied at different pH values. In vitro drug release of CCM was higher in the acidic medium (pH 5.5, 6.5) compared to physiological pH (7.4). The cytotoxicity of ZIF-8-GA, ZIF-8-GA-CCM, and ZIF-8-GA-CCM-FA structures was evaluated by the standard 3-(4,5 dimethylthiazol-2-yl)-2,5-diphenyltetrazolium bromide (MTT) assay on the three cell lines (fibroblast (normal cell), Hela (FR-positive), and A549 (FR-negative). These results suggested that the ZIF-8-GA-CCM-FA framework can have a promising effect on the targeted treatment of cancer cells.

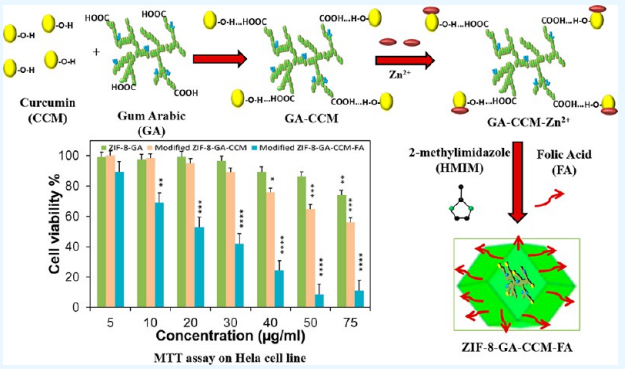

INTRODUCTION

Cancer is one of the dangerous diseases in the world. It reveals lots of varieties and complexity concerning different types of cells, physiological distinctiveness, and extracellular matrices that limit the efficiency of cancer therapy.[1] Also, large numbers of anticancer therapeutic agents are unstable and/or insoluble in water media. For solving these problems, drug delivery systems (DDSs) were proposed which can offer multiple benefits such as drug protection from degradation, enhancement of biocompatibility, and also reduction of drug side effects and doses by their effective delivery to the disease site.[2] Numerous drug carriers containing micelles, dendrimers,[3] liposomes,[4] nanomaterials,[5−8] hydrogels,[9] and metal organic frameworks[5] (MOFs) with different particle sizes and topologies have been studied until now.[1] MOFs are constructed by connecting metal cations with organic linker molecules with strong bonds that can produce nanoporous structures with one, two, or three dimensions.[10] MOFs are considered as a favorable class of nanocarriers for drug delivery due to their ultrahigh surface area and porosity, well-defined structure, tunable pore size, and easy chemical functionalization.[11] Release of drugs from carriers is affected by different endogenous and exogenous factors. Some of the endogenous parameters are alteration of pH, temperature, and glutathione concentration.[1,12] For the design of pH-responsive nanocarriers, a more acidic environment of cancer tissues with respect to physiological tissues can play a key role.[13] For example, a lot of studies have been performed on zeolitic imidazolate framework-8 (ZIF-8) that is a kind of pH-sensitive MOF and made by connecting Zn^{+2} cations with imidazolate (HmIm)organic linkers.[14] Thus, the carrier destruction and drug release occur higher in acidic media compared to physiologic media.[1] However, as reported in the literature, ZIF-8 shows high toxicity at concentrations above 30 μg/mL which limits the application of this carrier for DDSs.[15] In our previous work, a new strategy was suggested for the synthesis

Received: October 18, 2022
Accepted: December 26, 2022
Published: January 12, 2023

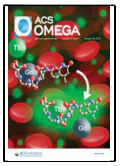

Scheme 1. Synthesis Procedure of ZIF-8-GA-CCM in Water At Room Temperature: (A) GA Aqueous Solution, (B) Formation of GA-CCM Complexes by the Addition of the Ethanoic Solution of CCM to the Aqueous Solution of GA, (C) Addition of Alkaline Solution of HmIm and the Solubility of GA-CCM, (D) Starting the Formation of ZIF-8-GA-CCM by Addition of Zn^{2+}, (E) Completion of the Formation of ZIF-8-GA-CCM after 15 min, and (F) ZIF-8-GA-CCM After Drying

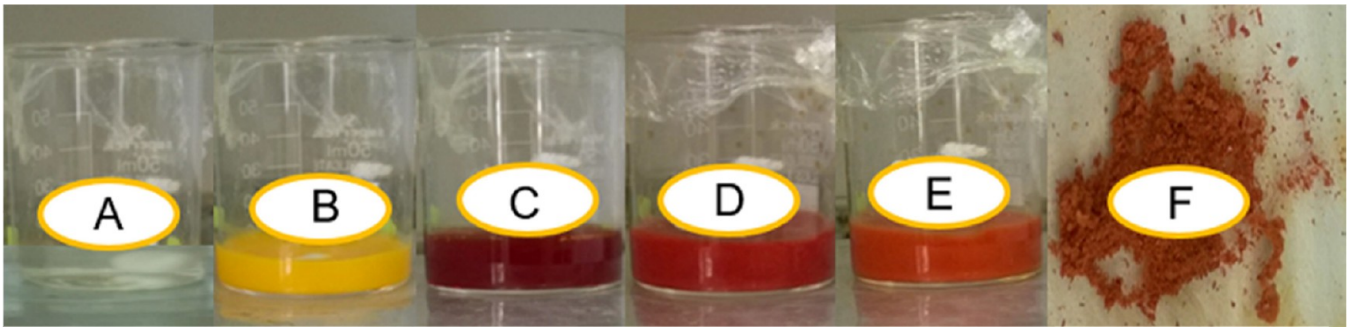

of biocompatible ZIF-8.[16] In this method, ZIF-8 was synthesized in the presence of gum arabic (GA) at room temperature in the aqueous medium, inspired by the natural biomimetic mineralization method (ZIF-8-GA). Recently, the biomineralization method was used for the encapsulation of some bioactive molecules such as polysaccharides, DNA, proteins, enzymes cells, and so on within the protective exterior layer.[17−21] GA is a type of heterogeneous polysaccharide that is obtained from acacia trees with a lot of advantages such as biocompatibility, nontoxicity, and high water solubility. This branched polysaccharide contains arabinose, rhamnose, galactose, and glucoronic acid residues.[22,23] Thus, the mentioned nanocarrier (ZIF-8-GA) showed more biocompatibility than ZIF-8. The nontoxic concentration of ZIF-8-GA was 70 μg/mL compared to 30 μg/mL for ZIF-8 as obtained by MTT assay.[16]

Curcumin (CCM) is a natural polyphenolic compound extracted from turmeric having anticancer, antioxidative, anti-inflammatory, anti-HIV, and antiangiogenic therapeutic properties, but it has some barriers like poor solubility in aqueous media and fast degradation in the physiological pH.[24,25] Consequently, the design of an effective DDS with high bioavailability and selective targeting for cancer cells is required for solving these problems. As reported in the literature, MOFs such as ZIF-8,[1,26] ZIF-67,[26] ZIF-L,[27] CD-MOFs,[28] and MIL-101(Fe)[29] were used for the delivery of CCM. Most of these syntheses were performed in organic solvents by time-consuming methods without using targeting agents.[1,29]

In this study, ZIF-8-GA was used as a nanocarrier for the delivery of CCM as an anticancer agent. This drug was encapsulated in the ZIF-8-GA nanocarrier (ZIF-8-GA-CCM) by using a one-pot method in an aqueous medium with a minimum amount of ethanol at room temperature. Also, for the targeted delivery of CCM to cancer cells with over-expressing folic acid (FA) receptors, the ZIF-8-GA-CCM nanocarrier was functionalized by FA. The ZIF-8-GA-CCM-FA nanocarrier was synthesized by a similar method with ZIF-8-GA-CCM only by the addition of FA to the synthesis medium. FA is water insoluble and can dissolve in some organic solvents or alkaline media. The synthesis of most of the functionalized DDSs with FA was done in organic toxic solvents and also in the separate process.[30−32] In our work, for the first time, FA was dissolved in water by using the alkaline property of the HmIm solution. The characterization techniques containing field-emission scanning electron microscopy (FESEM), X-ray diffraction (XRD), Fourier transform infrared (FTIR), UV−vis spectroscopy, and Brunauer−Emmett−Teller (BET) surface area analysis techniques were used in order to confirm the results. Also, the standard 3-(4,5 dimethylthiazol-2-yl)-2,5-diphenyltetrazolium bromide (MTT) assay was performed on the Fibroblast (normal cell), A549 (with negative folate receptor), and Hela (with positive folate receptor) cell lines in order to analyze the cytotoxicity of the ZIF-8-GA, ZIF-8-GA-CCM, and ZIF-8-GA-CCM-FA frameworks.

EXPERIMENTAL SECTION

Chemicals. Zinc acetate dihydrate ($Zn(OAc)_2{\cdot}2H_2O$, 98%), 2-methyl imidazole (HmIm,99%), and GA were purchased from MERCK. Phosphate buffer saline (PBS) and Dulbecco's modified Eagle's medium (DMEM) were purchased from Sigma-Aldrich. CCM (95%) was received from JinTai biological Company in China as a test sample. Materials for the MTT assay were purchased from Sigma-Aldrich. All chemicals were used without any further purification. Water used in all the experiments was distilled water. The Hela, A549, and human normal fibroblast cell lines were purchased from Pasteur Institute of Iran.

Synthetic Procedures. The synthesis of ZIF-8-GA-CCM was done as follows (Scheme 1): 6.0 mL of an aqueous solution of GA (150.0 mg) was prepared at room temperature (the solution was centrifuged in order to remove an excess amount of GA and provide a uniform solution) (Scheme 1A). To this solution, 2.0 mL of ethanolic solution of CCM (5.0 mg) was added. The yellow insoluble GA-CCM complexes were produced instantly, and the solution became opaque (Scheme 1B). Then, 3.0 mL of an aqueous solution of HmIm (561.0 mg) was added to the mixture. By this addition, the solution became transparent and red immediately (Scheme 1C). The color and transparency alterations were due to the solubility of the GA-CCM complex in the produced alkaline medium by the addition of HmIm solution. Finally, 1.0 mL of an aqueous solution of zinc acetate dihydrate (150.0 mg) was added. The opaque orange solution was obtained instantly (Scheme 1D). The HmIm linker/Zn^{2+} molar ratio was 10.0. After 15 min, the reaction completed (Scheme 1E), and the product was centrifuged and washed three times with water. The crystals of ZIF-8-GA-CCM were dried in a vacuum oven at 40 °C for 1 day (Scheme 1F). Some syntheses were performed for the comparison: (1) the same method was used for the synthesis of ZIF-8-GA-CCM containing 2.0 and 10.0

https://doi.org/10.1021/acsomega.2c06705
ACS Omega 2023, 8, 3245−3257

Scheme 2. Synthesis Procedure of ZIF-8-GA-CCM-FA in Water at Room Temperature and the Interaction between Components

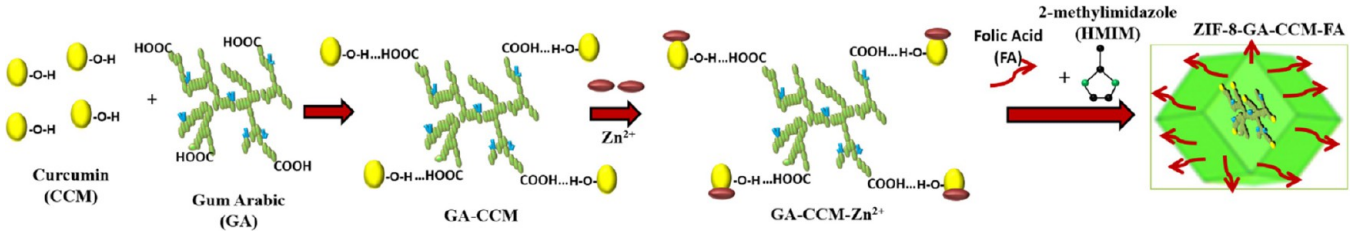

mg CCM; (2) the synthesis of ZIF-8-GA-CCM (5.0 mg CCM) was performed at 60 °C; higher temperature was employed to remove ethanol before addition of linker and metal precursor; (3) ZIF-8-CCM was prepared by a similar method without using GA; (4) ZIF-8-GA-CCM-FA frameworks containing 2.0, 5.0, and 10.0 mg of CCM were synthesized with the same method in the presence of FA. In these syntheses, 3.0 mL of aqueous solution of HmIm (561.0 mg) containing 10.0 mg of completely dissolved FA was used (Scheme 2); (5) after the production of ZIF-8-GA-CCM or ZIF-8-GA-CCM-FA containing 5.0 mg of CCM, whole of the obtained product was dispersed in 10.0 mL of PBS (pH = 7.4), and then 2.0 mL of ethanolic solution of 4.0 mg/mL CCM was added dropwise to the product dispersion and stirred for 3 min.This step was done for increasing the loaded drug without framework morphology alteration; these frameworks were named modified ZIF-8-GA-CCM and modified ZIF-8-GA-CCM-FA; (6) ZIF-8-GA was produced by using a similar procedure; then 6.0 mL of an aqueous solution of GA (150.0 mg) was provided. The solution was centrifuged in order to remove an excess amount of GA for the production of a uniform solution. Two prepared aqueous solutions of zinc acetate dihydrate (150.0 mg, 3.0 mL) and HmIm (561.0 mg, 3.0 mL) were added simultaneously to the GA solution (total solution volume: 12.0 mL and HmIm Linker/Zn^{2+} molar ratio: 10.0) and (7) ZIF-8 with a similar method without GA and CCM.

Characterization Techniques. FESEM images were obtained by a Hitachi S-4160 at an accelerating voltage of 20 kV. SEM analysis was performed with a TESKAN-Vega 3. XRD patterns were obtained by using a D8 ADVANCE type (BRUKER-Germany) with Cu-Kα radiation (λ = 0.1542 nm). The XRD patterns were taken with an angular step of 0.02°, with a sampling time of 1 s per step in the range of 2Θ [5−50°]. The absorbance measurements were performed using a Shimadzu 1601 PC UV−vis spectrophotometer. FTIR spectra were obtained by tensor II (BRUKER-Germany). TGA was performed by a TGA/DSC 1−Thermogravimetric Analyzer that was made by Mettler-Toledo International Inc. under a nitrogen atmosphere from room temperature to 800 °C with a heating rate of 5 °C min^{-1}. BET analysis was performed using a Micromeritics (USA), ASAP 2020 instrument. Absorbance of the solution for MTT assay was recorded by plate reader Polar Star Omega, BMG LABTECH, Germany instrument.

MTT Assay. Cytotoxicity was evaluated using the Fibroblast (normal cell), A549 (with negative folate receptor) and Hela (with positive folate receptor) cell lines. For this propose, each cell line was subcultured in complete media containing high glucose DMEM supplemented with 10% heat-inactivated fetal bovine serum in the presence of 1% penicillin/streptomycin at 37.0 °C under a humidified atmosphere of 5% CO_2. After reaching 90% of cell confluency, cells were detached using 0.25% prewarmed trypsin. Then, 1.0 × 10^4 of Hela and A549 cells and 1.5 × 10^4 cells/well of normal skin fibroblast were seeded into 96-well plates overnight in the above condition. In the next day, the medium was replaced with 100 μL of fresh culture medium containing 5.0, 10.0, 20.0, 30.0, 50.0, 75.0, and 100.0 μg mL^{-1} of different types of ZIF-8-GA-CCM. CCM treatment with final concentrations of 280.0, 140.0, 70.0, 35.0, 17.5, 8.7, and 4.4 μg/mL was also performed using 1% DMSO as the negative control. After 24, 48, and 72 h of incubation, cells were washed two times with PBS and incubated in a fresh medium containing 0.5 mg mL^{-1} of MTT solution. The plates were covered by aluminum foil and incubated in an incubator under CO_2 pressure for 4 h. Thereafter, the culture medium was removed, and the formazan crystals were dissolved in 100.0 μL of solubilization solution (40.0% (v/v) DMF, 16.0% (w/v) SDS, pH ∼ 4.7). Finally, the absorbance of the solution was recorded at a wavelength of 570 nm via a plate reader instrument. The cell viability was determined as follows:

$$\text{Cell Viability (\%)} = \frac{\text{A Sample} - \text{A Blank}}{\text{A Negative Control} - \text{A Blank}} \times 100$$

RESULTS AND DISCUSSION

Investigation of the Effect of Different Synthesis Conditions on ZIF-8-GA-CCM and ZIF-8-GA-CCM-FA. ZIF-8-GA was used for the in situ encapsulation of CCM and CCM/FA with different methods.

Investigation of the Effect of Temperature on the Synthesis of ZIF-8-GA-CCM. In order to find the best method for the in situ encapsulation of CCM in the ZIF-8-GA nanocarrier, FESEM analysis was performed. The synthesis of ZIF-8-GA-CCM was performed by two methods (1) at room temperature and (2) in an oil bath at 60 °C. Higher temperature was employed to remove the ethanol after preparation of the GA-CCM complex and before addition of the HmIm linker and metal precursor. Figure 1 shows the FESEM images of the synthesized products by using 5.0 mg of CCM by these two methods. As is obvious, the synthesized ZIF-8-GA-CCM at room temperature has more uniformity and a smaller size with an average size of 374 nm compared to the sample obtained at 60 °C with an average size of 492 nm based on the size distribution (Figure 1). As reported in the literature, the homogeneous phase of ZIF-8 crystals is a truncated rhombic dodecahedron.

Investigation of the Effect of GA on the Synthesis of ZIF-8-GA-CCM. ZIF-8-GA-CCM and ZIF-8-CCM were synthesized in the same condition at room temperature. In the case of ZIF-8-CCM, GA was not used in the synthesis

https://doi.org/10.1021/acsomega.2c06705
ACS Omega 2023, 8, 3245−3257

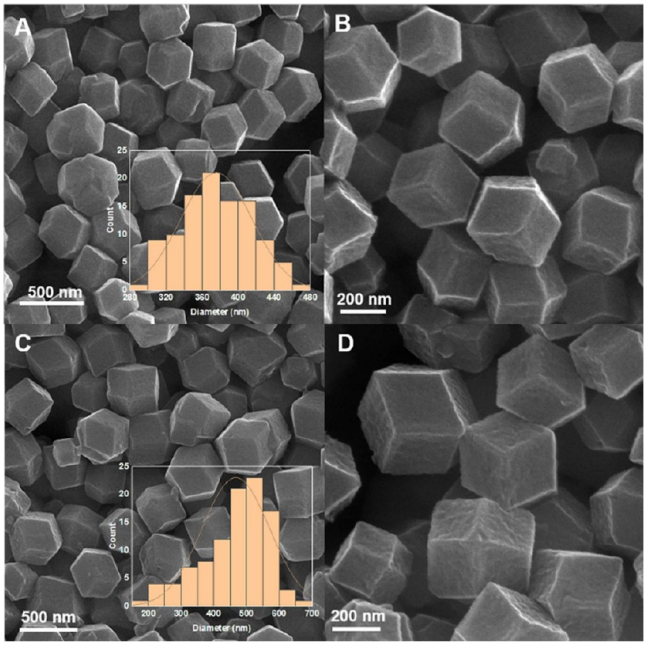

Figure 1. FESEM images of the synthesized ZIF-8-GA-CCM with two different methods (A and B) at room temperature and (C and D) in an oil bath at 60 °C. Insets: size distributions of samples.

medium. Figure 2 shows the FESEM images of ZIF-8-CCM and ZIF-8-GA-CCM. As is obvious, the homogeneous phase of

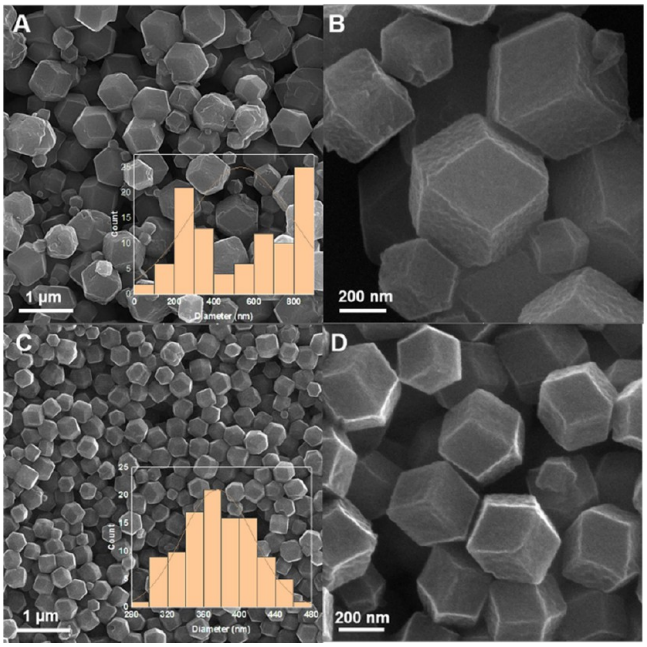

Figure 2. FESEM images of (A and B) ZIF-8-CCM and (C and D) ZIF-8-GA CCM. Insets: size distributions of samples.

ZIF-8 crystals, truncated rhombic dodecahedron, can produce in both conditions, but the presence of GA led to more uniformity and smaller mean particle size of the obtained crystals. The mean particle size of ZIF-8-CCM and ZIF-8-GA-CCM was 551 and 374 nm based on the size distribution, respectively (Figure 2). As reported in the literature, a natural polysaccharide such as starch and GA can form complex with CCM by using a facile solution mixing method. The interaction between −OH groups of CCM and−OH or −COOH group of polysaccharide by the hydrogen bonding can result in the formation of a complex.[33,34] Herein, also a complex can form between CCM and GA by hydrogen bonding (Scheme 2). The obtained CCM-GA complex had yellow color and good dispersion in water (Scheme 1B). On the other hand, CCM can chelate to di and trivalent inorganic ions such as Zn^{2+}, Al^{3+}, and Fe^{3+} and form metallo-complexes of CCM. For example, the interaction of CCM with Zn^{2+} (Scheme 2) can make a stable complex that is more soluble for transportation by blood stream and indicates greater therapeutic effects compared to CCM alone.[35] In our work, the complex of CCM-GA and also CCM-GA-Zn^{2+} can act as a template for the biomineralization process of ZIF-8 (Scheme 2). Thus, the produced ZIF-8-GA-CCM had more uniform sizes compared to ZIF-8-CCM (Figure 2).

Investigation of the Effect of CCM on the Synthesis of ZIF-8-GA-CCM. For the investigation of the effect of the amount of CCM on the particle size and morphology of the obtained products, different amounts of CCM containing 2.0, 5.0, and 10.0 mg were selected in the presence of 150.0 mg GA in a total volume of 12.0 mL at a linker/metal molar ratio of 10. Figure 3 shows the FESEM images of the crystals obtained with different amounts of CCM. By increasing the amount of CCM, the particle size decreased due to the elevated number of GA-CCM complex as a template in the synthesis medium (Figure 3A−C). The obtained product in the presence of 5.0 mg CCM had complete truncated rhombic dodecahedron morphology with an average size of 374 nm (Figure 3B). In the case of 2.0 mg CCM, the larger particles with no smooth and complete edges and faces with an average size of 469 nm were obtained compared to 5.0 mg CCM based on the size distribution (Figure 3A,B). For the CCM amount of 10.0 mg, the obtained crystals had rounded corners with an average size of 90 nm based on the size distribution (Figure 3C). For the investigation of the effect of postmodification of the synthesized framework with more CCM (5.0 + 8.0), its FESEM image was investigated. As shown in Figure 3D, the morphology and size of modified ZIF-8-GA-CCM were very similar to the framework with 5.0 mg of CCM. Also, the synthesis of ZIF-8-GA was performed without CCM. In this condition, a nonuniform product was obtained after 15 min (Figure 3E). At 24 h, the product had truncated rhombic dodecahedron morphology but with relatively wide size distribution and a large average size of 536 nm (Figure 3F). Also, the synthesized ZIF-8 in the absence of CCM and GA was much bigger with an average size of 708 nm compared to the ZIF-8-GA and ZIF-8-GA-CCM at 24 h (Figure S1). In this case, after 15 min, very low product was obtained based on the size distribution. The required time for completion of ZIF-8-GA-CCM synthesis was 15 min in comparison to 24 h for ZIF-8-GA and ZIF-8. As reported, the effective parameters on the synthesis of ZIF-8 with truncated rhombic dodecahedron morphology are linker/metal molar ratio, water amount, and presence of template.[16,36] The results showed the effect of the GA-CCM template on the formation of a more uniform and smaller ZIF-8 product and the facilitation of its kinetic of formation compared to GA alone.

Investigation of the Effect of FA on the Synthesis of ZIF-8-GA-CCM. FA can enhance the targeting capacity of nanocarriers due to its high affinity to the receptors which are overexpressed on the cancer cell surfaces compared to the normal cell.[31] FA presence in the synthesis medium can result

https://doi.org/10.1021/acsomega.2c06705
ACS Omega 2023, 8, 3245−3257

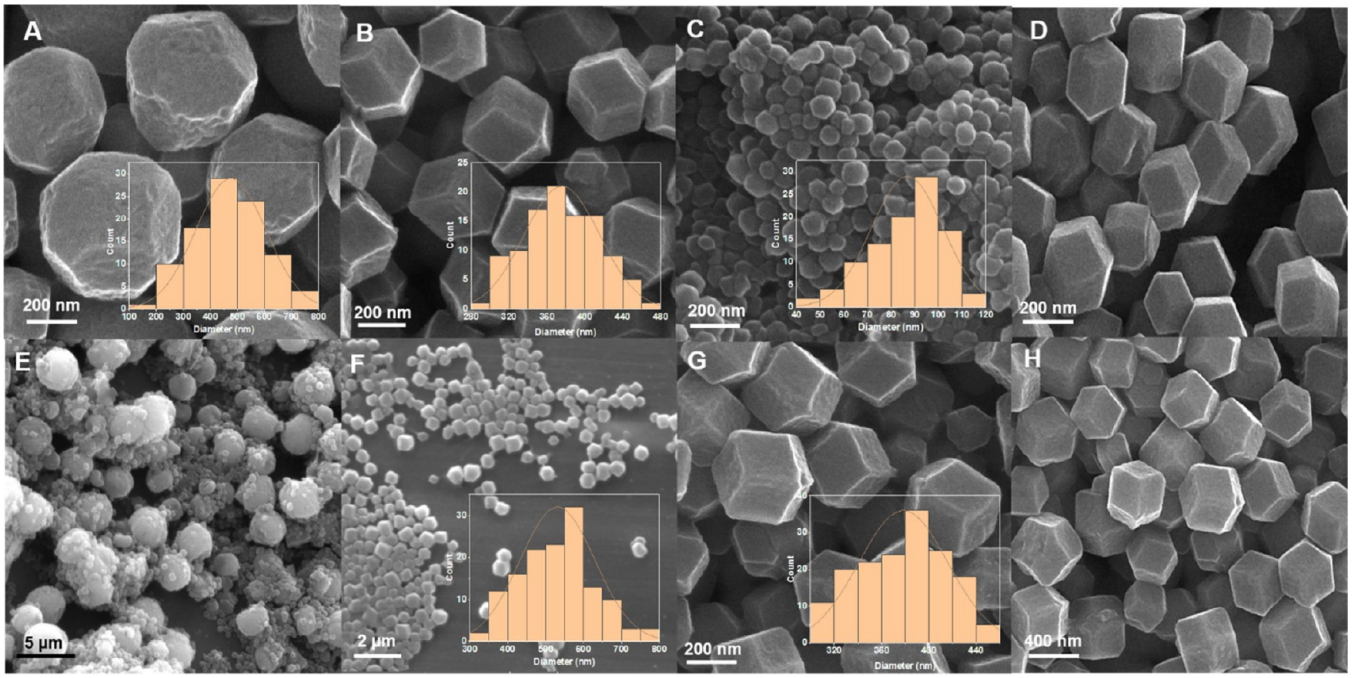

Figure 3. FESEM and SEM images of ZIF-8-GA-CCM at a linker/metal molar ratio of 10 in the presence of different amounts of CCM (A) 2.0 mg, (B) 5.0 mg, and (C) 10.0 mg after 15 min, (D) 8 + 5 mg (modified ZIF-8-GA-CCM), ZIF-8-GA without CCM after (E) 15 min and (F) 24 h at linker/metal molar ratio of 10, (G) ZIF-8-GA-CCM-FA at a linker/metal molar ratio of 10 in the presence of 5.0 mg of CCM and 10.0 mg of FA after 15 min, and (H) 8.0 + 5.0 mg CCM and 10.0 mg FA (modified ZIF-8-GA-CCM-FA). Insets: size distributions of samples.

in its encapsulation in the ZIF-8-GA-CCM framework. In our procedure, the encapsulation of FA was performed in one pot by using alkaline nature of HmIm in the aqueous medium for the first time without using any toxic organic solvents or conjugation agents. As shown in Figure 3, the morphology of ZIF-8-GA-CCM-FA did not alter compared to that of ZIF-8-GA-CCM. Its average size was 383 nm based on the size distribution (Figure 3). Also, postmodification of the synthesized framework with more CCM (5.0 + 8.0) had no effect on its morphology (Figure 3H).

Also, the crystallinity of the synthesized ZIF-8-GA-CCM and ZIF-8-GA-CCM-FAin the presence of 5.0 mg CCM was studied by XRD analysis (Figure 4). In two cases, the peaks at 2θ values of 7.29, 10.44, 12.83, and 18.10 were obtained which corresponded to (110), (200), (211), and (222) index planes,

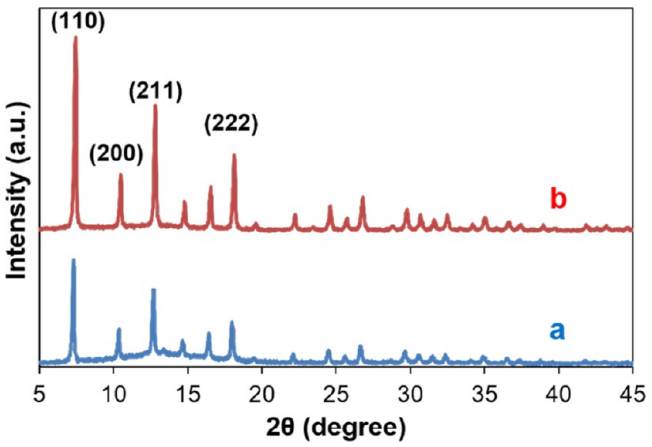

Figure 4. XRD analysis of (a) ZIF-8-GA-CCM and (b) ZIF-8-GA-CCM-FA.

respectively. These are the specific peaks of the homogeneous phase of ZIF-8 crystals with truncated rhombic dodecahedron morphology that reported in the literature.[36] The results confirmed the complete formation of the ZIF-8 framework in the presence of GA, CCM, and FA in the aqueous media. The synthesized MOFs were stable in a dry environment for several months. In the case of ZIF-8-GA-CCM and ZIF-8-GA-CCM-FA, a small uniform homogeneous phase was obtained in a linker/metal molar ratio of 10.0 in very short time at a volume of 12.0 mL compared to larger products acquired after 24 h for ZIF-8-GA. This decrease in the average size and reaction time can be related to the formation of the GA-CCM complex as the template in the synthesis medium before the preparation of the ZIF-8 framework. Also, the interaction between CCM and Zn^{2+} can be effective.[35]

Confirming the Presence of CCM in the ZIF-8-GA-CCM Framework. For confirming the presence of CCM in the ZIF-8-GA-CCM framework, some analyses were performed.

BET Analysis. The BET adsorption analysis was performed to obtain the surface area and porosity of one pot synthesized ZIF-8-GA-CCM-FA. Its BET isotherm is shown in Figure 5. At low relative pressure, the isotherm indicated the noteworthy enhancement in nitrogen adsorption; therefore, the ZIF-8-GA-CCM-FA isotherm is type-I (Langmuir isotherm) that verified its microporosity (Figure 5). The BET surface area, pore volume, and pore diameter of ZIF-8-GA-CCM-FA were 1353.23 $m^2\ g^{-1}$, 0.653 $cm^3\ g^{-1}$, and 19.29 Å, respectively. Because the same size ZIF-8 did not synthesize without CCM or CCM-GA in the same HmIm/Zn^{2+} molar ratio (Figure S1), it was not possible to compare its BET results with ZIF-8-GA-CCM-FA. The acquired results for ZIF-8-GA-CCM-FA were close to the reported amounts in the literature.[36−39] Due to the common small pore size of ZIF-8, in situ drug encapsulation

https://doi.org/10.1021/acsomega.2c06705
ACS Omega 2023, 8, 3245−3257

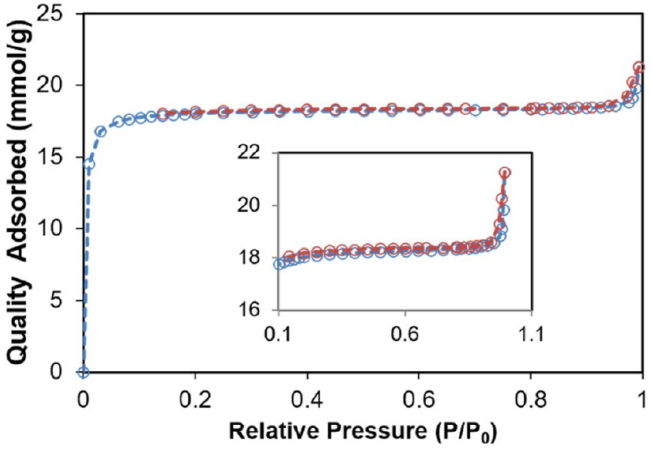

Figure 5. Nitrogen adsorption−desorption isotherm of ZIF-8-GA-CCM-FA.

can be the best choice for increasing drug loading compared to the postsynthesis method.[39,40]

FT-IR Analysis. The ZIF-8-GA, ZIF-8-GA-CCM, ZIF-8-GA-CCM-FA, free CCM, and free FA were analyzed by FT-IR (Figure 6). The observed peaks at 422, 694, 1146, 1300−1460,

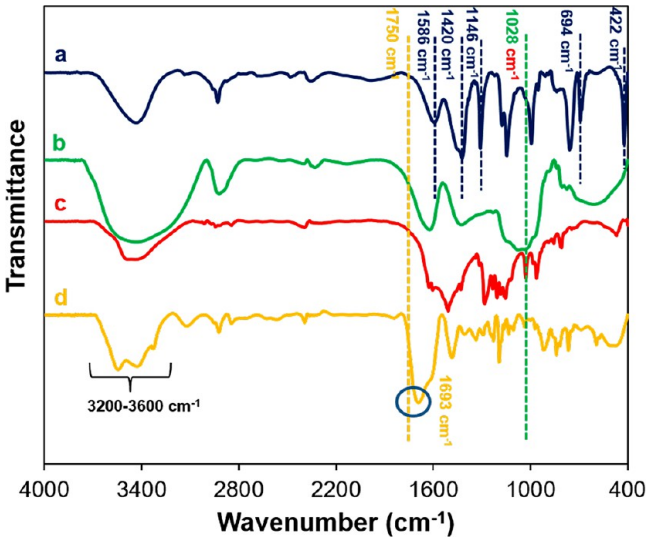

Figure 6. FTIR spectra of (a) ZIF-8-GA-CCM-FA, (b) GA, (c) CCM, and (d) FA.

and 1585 cm^{-1} can be related to Zn−N stretching vibration, ring out of plane bending vibration, the aromatic C−N stretching, the whole ring stretching, and aromatic C=N stretching modes of HmIm, respectively (Figure 6a). These peaks confirmed the formation of ZIF-8 in the presence of GA, CCM, and FA in very short reaction time and a linker/metal molar ratio of 10 at a volume of 12.0 compared to previously reported studies.[36] In the case of GA, CCM, and FA, most of the vibrations were common between them and overlapped (Figure 6b−d). The observed peak at 1028 cm^{-1} can be related to C−O and C−O−C stretching mode of GA, CCM, and FA in the ZIF-8-GA-CCM-FA framework (Figure 6).[1,41,42] Also, the detected peak at 1750 cm^{-1} indicated the C=O amide stretching of the alpha carboxyl group of FA (Figure 6a). This peak had been shifted compared to the corresponding peak of free FA at 1693 cm^{-1} that can be due to its interaction in the framework (Figure 6d).[43] The peaks in the range of 3200−3600 cm^{-1} can be related to O−H stretching modes of GA, CCM, and FA (Figure 6).[41−43]

As reported in the literature, the existence of various hydroxyl groups on the polysaccharides such as GA and also CCM drug plays an essential role in the biomimetic mineralization process due to the coordination interaction between the oxygen-containing functional groups such as O−H of GA-CCM and Zn^{2+} ions. This interaction caused the enhancement of the local concentration of Zn^{2+} and helped the ZIF-8 nucleation round the GA-CCM.[17]

UV−Visible Analysis. UV−visible spectroscopy was used for the analysis of the absorption peaks of GA, free CCM, ZIF-8-GA, and also ZIF-8-GA-CCM frameworks synthesized with 5.0 and 10.0 mg of CCM and 150.0 mg of GA in the total volume of 12.0 mL. Figure 7 shows their UV−visible spectra in

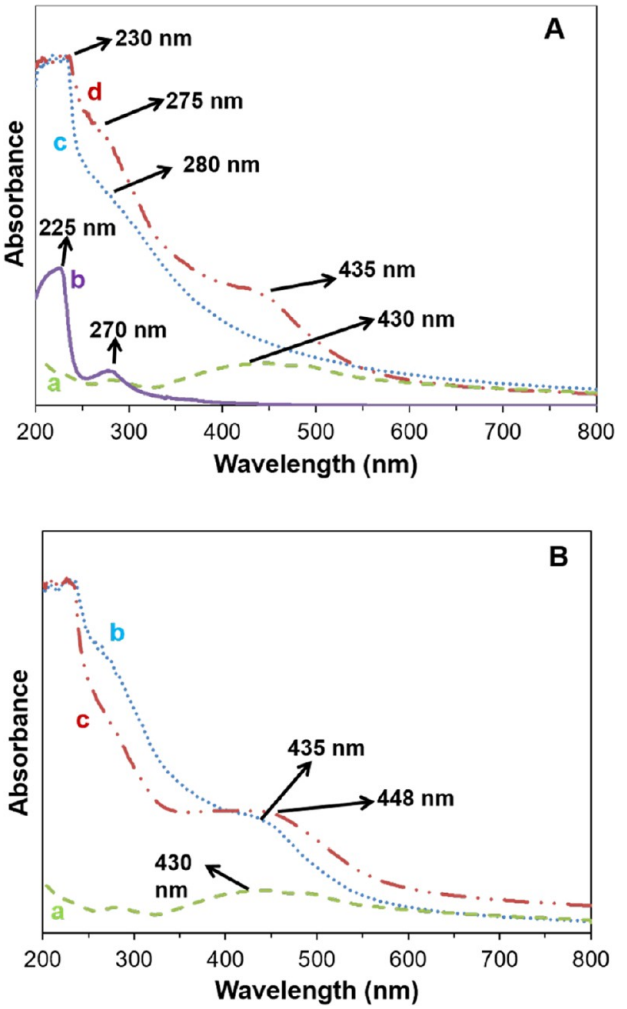

Figure 7. Comparison of the UV−vis spectra of (A) free CCM (a), free GA (b), ZIF-8-GA (c) and ZIF-8-GA-CCM (5.0 mg) (d) and (B) free CCM (a), ZIF-8-GA-CCM (5.0 mg) (b) and ZIF-8-GA-CCM (10.0 mg) (c).

the range of 200−800 nm. Based on the literature, ZIF-8 and GA have one and two corresponding peaks that were, in our case, observed at 211, 225, and 270 nm, respectively (Figure 7Ab).[16] The detected peaks of GA in the ZIF-8-GA and ZIF-8-GA-CCM framework had a red shift compared to free GA that indicated the encapsulation of GA and its corresponding

https://doi.org/10.1021/acsomega.2c06705
ACS Omega 2023, 8, 3245−3257

interactions in the framework (Figure 7Ac,d).[16] Free CCM showed the absorption peak at 430 nm (Figure 7Aa) that shifted to the higher wavelength in the ZIF-8-GA-CCM framework (435 nm) (Figure 7Ad). The result confirmed the encapsulation of CCM in the ZIF-8-GA framework. The observed shift can be related to the formation of GA-CCM and CCM-Zn complexes that led to the alteration of the absorption peak of the CCM in the framework. Also, the shift of the CCM peak in the framework enhanced by increasing the amount of CCM. Figure 7B shows the UV−visible spectra of ZIF-8-GA-CCM with 5.0 and 10.0 mg of CCM and free CCM. This comparison showed that the wavelength of the CCM peak shifted to a higher amount due to the increase of CCM from 5.0 to 10.0 mg (Figure 7Bb,c).

Investigation of the Dispersion Capability of the ZIF-8-GA-CCM, GA-CCM Complex, and Free CCM in Water. For investigation of the dispersion capability of the free CCM, GA-CCM complex, and the ZIF-8-GA-CCM, the specific amount of each sample was dispersed in 10.0 mL of water. Figure 8 shows the pictures of dispersion of these samples in water. The dispersion capability of the free CCM was very low in the water (Figure 8a). While the GA-CCM complex and ZIF-8-GA-CCM were dispersed completely in water (Figure 8b,c). The results showed the effect of GA with so many hydrophilic groups containing hydroxyl, amino, and carboxyl groups on the dispersion of the hydrophobic samples like CCM and ZIF-8.[16,23] As reported in the literature, the natural polysaccharide can form a complex with CCM by the interaction between OH groups of CCM and polysaccharide by the hydrogen bonding (Scheme 2).[23] This interaction can lead to good dispersion of these complexes in water compared to free CCM or ZIF-8.[33] On the other hand, formation of the CCM-Zn^{2+} complex in the ZIF-8-GA-CCM (Scheme 2) can enhance its dispersion in water.[35] Thus, ZIF-8-GA can be a convenient delivery vehicle for CCM with poor water-solubility and rapid degradation under physiological conditions.[40]

Figure 8. Picture of dispersion of (A) free CCM, (B) GA-CCM complex, and (C) ZIF-8- GA-CCM in water.

Calculation of the Drug Loading Capacity (DLC) and Drug Loading Efficiency (DLE) Percentage. As reported in the literature, ZIF-8 is a good pH-responsive drug delivery vehicle; however, the pore size of nanoporous ZIF-8 is smaller than that of most drug molecules. In the postsynthesis drug loading method, drug molecules are commonly adsorbed on the surface of the MOF, causing their low loading.[39,40] Herein, the one-pot method was applied for increasing the CCM encapsulation during the ZIF-8 synthesis process. For determination of DLE% and DLC% of CCM, in the first step, the standard calibration curve of the CCM in ethanol was obtained (Figure S2), and the following equation was achieved:

$$Y = 0.064X + 0.009$$

In this equation, X is the CCM concentration in μg/mL and Y is the amount of the absorption of CCM at a wavelength of 430 nm. Two milligrams of the ZIF-8-GA-CCM was decomposed in 50.0 μL of HCL and diluted to 2.0 mL with ethanol. Then, the absorption amount of the CCM in this solution after 5 times dilution was read by the plate reader device and was 0.415. Based on the above equation, the concentration of the CCM was 32.93 μg/mL. In other words, the amount of CCM in the 1000 μg ZIF-8-GA-CCM nanostructure was 33.0 μg, approximately. Also, the total amount of ZIF-8-GA-CCM was almost 137.0 mg, and the amount of free CCM was 5.0 mg. Therefore, the amount of DLC and DLE was calculated by the following equation:

$$\text{DLE}(\%) = (\text{amount of loaded drug}) / (\text{total amount of feeding drug}) \times 100$$

$$\text{DLC}(\%) = (\text{amount of loaded drug}) / (\text{amount of drug loaded NPs}) \times 100$$

By using these equations, DLE% and DLC% of CCM in this sample were 90 and 3.3%, respectively. The results showed that CCM was successfully loaded in the ZIF-8-GA framework. As said above, one-pot loading of the drug in the MOF synthetic medium leads to the encapsulation of the drug with the best efficiency.[44−46]

Investigation of the Performance of Nanocarriers in the Drug Delivery. To investigate the releasing kinetics of CCM from ZIF-8-GA-FA, its de-polymerization was studied in acidic pH (pH = 5.5 and 6.6) compared to the neutral condition (pH = 7.4) which denoted the secondary endosome, tumor microenvironment, and blood normal condition pH values, respectively. As illustrated in Figure 9A−C, the UV−visible spectrum showed its faster rate of release from the framework under the acidified condition compared to normal blood circulation. This can be mainly due to the breaking of the attachment between Zn^{2+} ions and HmIm in the framework in the acidic environment by competition between protons and Zn^{2+} ions trying to coordinate with HmIm.[47] This led to CCM-enhanced release in the acidic medium and reduced release under physiological conditions due to different ZIF-8 decomposition. The cumulative release of CCM was drawn based on percentage (Figure 9D) and ppm (Figure S3) vs time (h). According to the data, 72% (5.9 ppm) and 60% (4.6 ppm) of CCM were released after 24 h in the acidic environment, at pH 5.5 and 6.6, respectively, while unwanted leakage at normal pH reached 43% (3.5 ppm) after 24 h.

Also, SEM analysis of ZIF-8-GA-CCM-FA after 72 h of incubation in mentioned pH values (7.4, 6.5, and 5.5) showed the morphological disruption of the rhombic dodecahedron framework to layered structure in the acidified environment compared to the neutral condition which is reported earlier (Figure 10).[16]

https://doi.org/10.1021/acsomega.2c06705
ACS Omega 2023, 8, 3245−3257

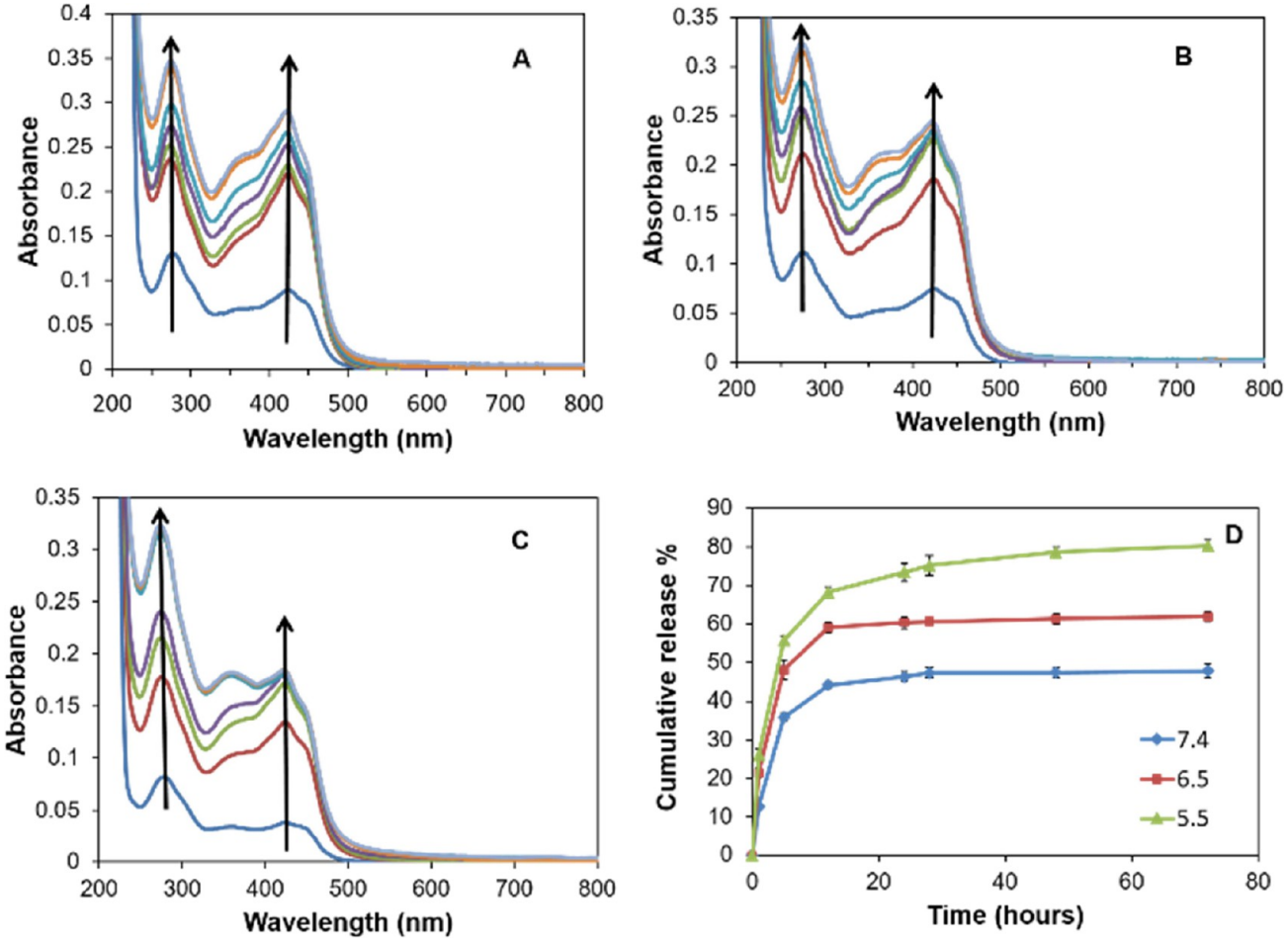

Figure 9. UV−visible spectra of CCM released from ZIF-8-GA-CCM-FA framework at pH (A) 5.5, (B) 6.5, and (C) 7.4 in PBS. (D) In vitro relative releasing profile of CCM from ZIF-8-GA-CCM-FA after 72 h of incubation. Kinetic release data are presented as the average ± SD (n = 3) in three independent experiments.

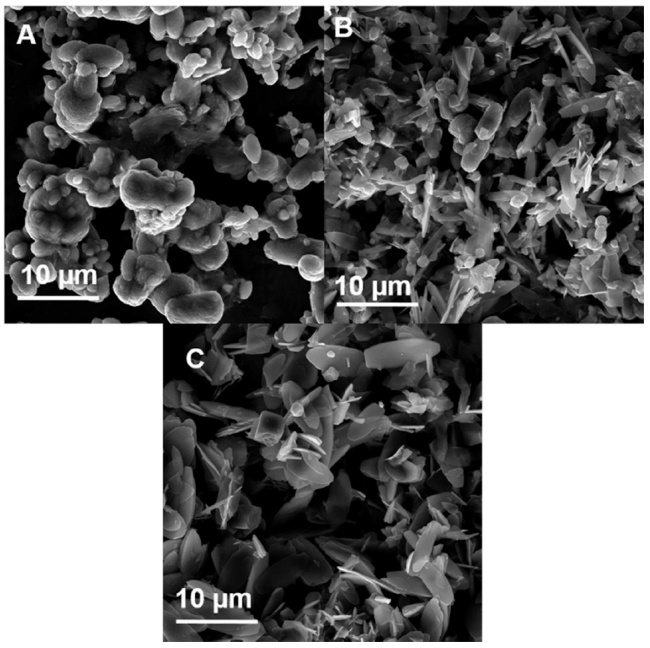

Figure 10. SEM images of ZIF-8-GA-CCM-FA after 72 h of incubation in PBS buffer, pH (A) 7.4, (B) 6.5, and (C) 5.5.

Cytotoxicity Studies. The newly synthesized ZIF-8-GA nanocarrier was used as a delivery vehicle for the anticancer model drug, CCM. ZIF-8-GA was also functionalized with FA to enhance targeting ability of the framework against overexpressed tumor-associated antigen, FA receptor, which is mainly detected on a wide variety of cancer cells including breast, ovarian, lung, kidney, brain, endometrial, and colon cancer.[48−50] As reported previously, the ZIF-8-GA framework indicated greater biocompatibility against normal cells up to 75 μg/mL compared to the parental structure, ZIF-8 with a toxicity threshold of 30 μg/mL.[16] As reported in the previous work, the enhanced biocompatibility of ZIF-8-GA can be due to the antioxidant property of GA by the reduction of ROS amount with chelation of released Zn^{2+}. In the second step, the anticancer ability of different amounts of CCM (5.0, 10.0 , and 5.0 + 8.0 mg) loaded ZIF-8-GA and ZIF-8-GA-FA on three cell lines, Hela (as an FA positive receptor), A549 (as an FA negative receptor), and skin fibroblast (as a normal cell line) was investigated (see supplementary Figures S4−S6). Fibroblasts as normal cell lines are the most widespread cells used in the cell culture investigations and are easy to culture. In addition, instead of the blood, every tissue of the body contains fibroblast cells.[51] Different loading concentrations of CCM on ZIF-8-GA and ZIF-8-GA-FA showed biocompatibility against normal fibroblasts up to 75 μg/mL except for 72 h of incubation of ZIF-8-GA-FA with 10 and 5.0 + 8.0 mg of CCM

https://doi.org/10.1021/acsomega.2c06705
ACS Omega 2023, 8, 3245−3257

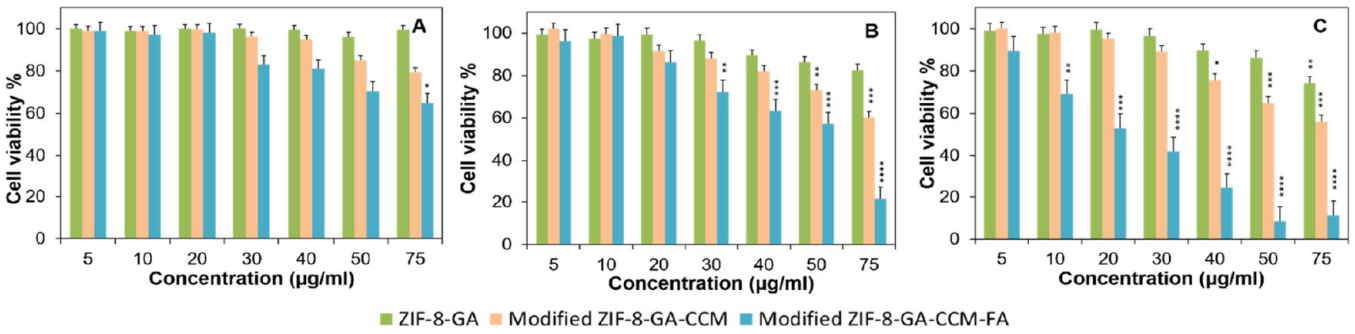

Figure 11. In vitro toxicity analysis of ZIF-8-GA, modified ZIF-8-GA-CCM, and modified ZIF-8-GA-CCM-FA networks at (A) 24, (B) 48, and (C) 72 h of incubation against HeLa cell lines. All data are displayed as the average ± SD (n = 3). The statistical evaluation was performed using the t-test with *(P-value ≤0.05), **(P-value ≤0.01), ***(P-value ≤0.001), and ****(P-value ≤0.0001) significance values.

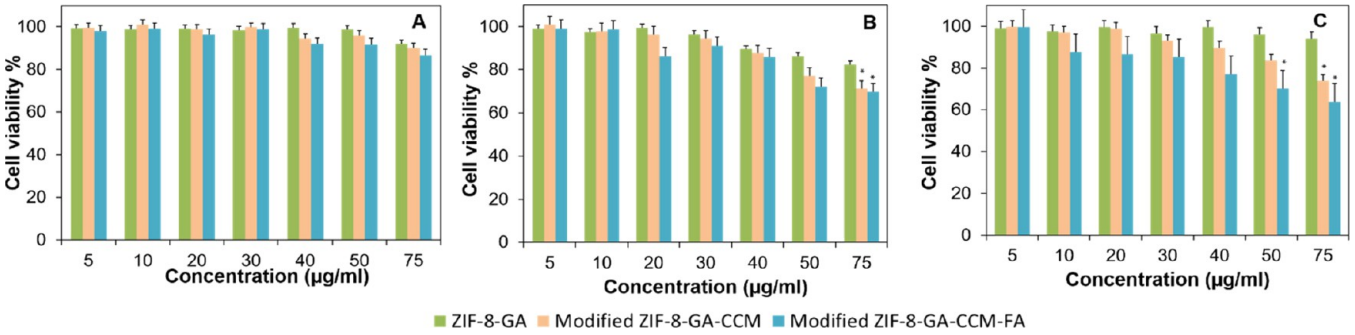

Figure 12. In vitro toxicity analysis of ZIF-8-GA, modified ZIF-8-GA-CCM, and modified ZIF-8-GA-CCM-FA networks at (A) 24, (B) 48, and (C) 72 h of incubation against skin fibroblast cells. All data are displayed as the average ± SD (n = 3). The statistical evaluation was performed using the t-test with *(P-value ≤0.05), **(P-value ≤0.01), ***(P-value ≤0.001), and ****(P-value ≤0.0001) significance values.

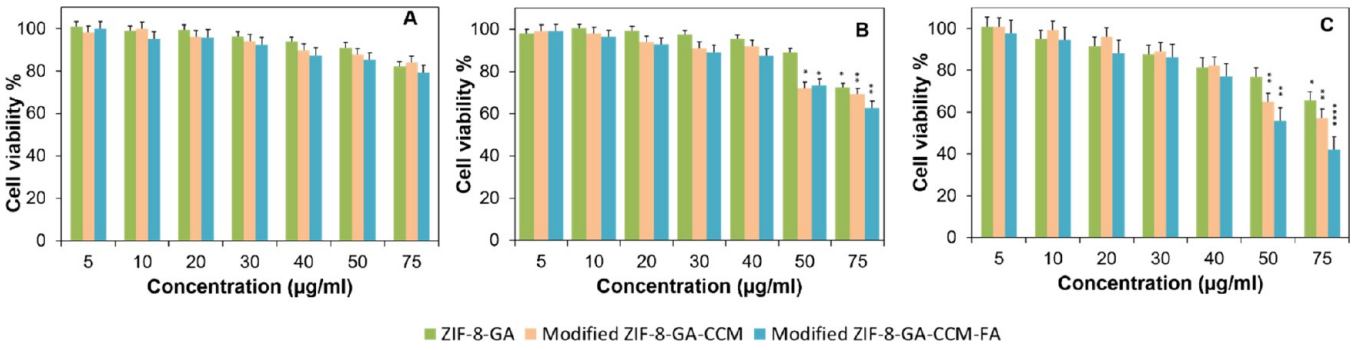

Figure 13. In vitro toxicity analysis of ZIF-8-GA, modified ZIF-8-GA-CCM, and modified ZIF-8-GA-CCM-FA networks at (A) 24, (B) 48, and (C) 72 h of incubation against A549 cell lines. All data are displayed as the average ± SD (n = 3). The statistical evaluation was performed using the t-test with *(P-value ≤0.05), **(P-value ≤0.01), ***(P-value ≤0.001), and ****(P-value ≤0.0001) significance values.

compound. In addition, the combination loading of in situ and postadsorption of CCM on modified ZIF-8-GA-CCM-FA represented excellent anticancer activity on the FA positive cell, HeLa, compared to FA negative cell, A549. Therefore, nanocarrier ZIF-8-GA and ZIF-8-GA-FA containing 5.0 + 8.0 mg of CCM were selected for further analysis. As illustrated in Figures 11−13, their cytotoxicity against three different cell lines were shown up until 72 h of incubation and compared with ZIF-8-GA without CCM. As illustrated in Figure 11, 10 μg/mL of modified ZIF-8-GA-CCM-FA showed significant cellular effects with the maximum effects on 50 μg/mL against positive FA receptor, Hela, cell lines with an inhibitory percentage of 89% after 72 h of incubation. Between modified ZIF-8-GA-CCM and ZIF-8-GA-CCM-FA, later showed higher cytotoxicity on Hela cells that confirmed the effect of FA for targeted delivery of CCM. In return, ZIF-8-GA, modified ZIF-8-GA-CCM, and ZIF-8-GA-CCM-FA were safe on normal and A549 cells up to 40 μg/mL after 72 h incubation in which their viabilities were calculated to be 100, 96, and 80% on normal cells and 98, 90, and 78% on A549 cells (Figures 12 and 13). The IC50 values of ZIF-8-GA-CCM and ZIF-8-GA-CCM were also calculated (Figure S7). The selective index (SI) was calculated in order to investigate the improvement of effectiveness of the designed drug delivery system. SI is the IC_{50} normal cell/IC_{50} cancerous cell that was calculated for different samples in 72 h. The more SI values can show the higher biocompatibility of the nanocarrier. According to Table 1, ZIF-8-GA-FA harboring 5.0, 10.0, and 5.0 + 8.0 mg of CCM improved the performance of CCM compared to free CCM on the FA positive cell, HeLa, with SI values of 1.66, 1.23, and 2.70, respectively. SI value comparison of ZIF-8-GA-CCM and ZIF-8-GA-CCM-FA showed that FA acted effective for

https://doi.org/10.1021/acsomega.2c06705
ACS Omega 2023, 8, 3245−3257

Table 1. SI of Free CCCM, ZIF-8, ZIF-8-GA and different CCM loaded ZIF-8-GA and ZIF-8-GA-FA after 72 h of Incubation[a]

sample	SI = $IC_{50normal}/IC_{50H}$	SI = $IC_{50normal}/IC_{50A}$
free CCM	1.20	1.50
ZIF-8	0.94	0.93
ZIF-8-GA	1.00	1.00
ZIF-8-GA-CCM (5 mg)	1.04	1.00
ZIF-8-GA-CCM-FA (5 mg)	1.66	1.05
ZIF-8-GA-CCM (10 mg)	1.01	1.00
ZIF-8-GA-CCM-FA (10 mg)	1.23	0.85
ZIF-8-GA-CCM (5 + 8 mg)	1.00	1.00
ZIF-8-GA-CCM-FA (5 + 8 mg)	2.70	0.78

[a]Those nanocarriers that did not reach to 50% cell inhibitory concentration was kept at maximum concentration, 75 μg/mL.

increasing the selectivity of the nanocarrier between normal and FA positive cancerous cells. In contrast, SI values against A549 cell lines (folic acid negative) were reduced from 1.054 to 0.78 by increasing CCM concentration in the ZIF-8-GA-CCM-FA framework.

Cellular Uptake Study. The specific cellular accumulations of autofluorescent CCM were also investigated using fluorescence microscopy.

As shown in Figure 14, the 24 h of cytoplasmic accumulations of free CCM, modified ZIF-8-GA-CCM, and modified ZIF-8-GA-CCM-FA were presented. As shown in Figure 14A−C, the accumulation of free CCM was noticed in all cell lines which means that CCM did not show any selectiveness entrance inside the cells. In contrast, both ZIF-8-GA-CCM and ZIF-8-GA-CCM-FA showed slower accumulation that showed controlled entrance of CCM into the cells. Also, the fluorescence intensity of CCM showed that the presence of FA improved the targeting of modified ZIF-8-GA-CCM-FA on Hela cells with positive FA receptor compared to A549 and normal skin fibroblast cells.

CONCLUSIONS

In this study, we suggested a new nanocarrier (ZIF-8-GA) for one-pot encapsulation of an anticancer CCM drug. Targeting of ZIF-8-GA-CCM with FA was done in the aqueous medium at room temperature by the alkaline pH produced by a HmIm linker without using any toxic organic solvent or additional conjugation agents. All the characteristic analyses confirmed the effective synthesis of ZIF-8-GA-CCM andZIF-8-GA-CCM-FA structures with a truncated rhomboid dodecahedron shape in the aqueous medium at room temperature. The presence of GA and CCM not only reduced the size of formed ZIF-8 but also the synthesis time to 15 min. These can be due to the presence of the Zn^{2+}-CCM-GA complex as a template in the ZIF-8 synthesis process. The obtained structures were smaller, uniform, and water-dispersible compared to the many reported studies. The presence of GA in ZIF-8-GA led to its more biocompatibility and hydrophilicity compared to ZIF-8 due to the functional groups of GA. Also, the poor water-solubility and rapid degradation of CCM under physiological conditions were improved by its loading in the ZIF-8-GA carrier because of its interaction with functional groups of GA and also complexation with Zn^{2+}. The ZIF-8-GA-CCM-FA framework was pH-responsive. In vitro drug release of CCM was higher in the acidic medium (pH 5.5 and 6.5) compared to physiological pH (7.4). This can be mainly due to the breaking of the attachment between Zn^{2+} ions and HmIm in the framework in the acidic environment by competition between protons and Zn^{2+} ions trying to coordinate with HmIm. This MOF is a

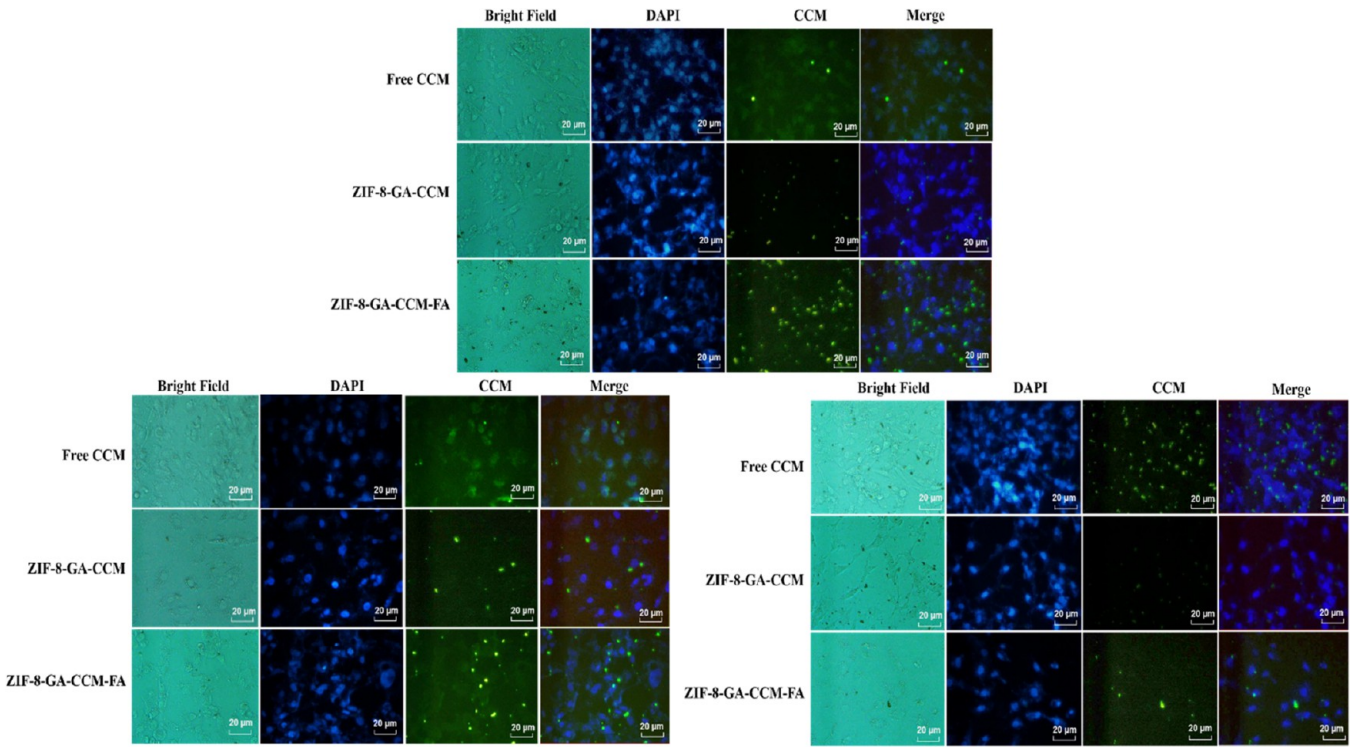

Figure 14. Fluorescent images of free CCM, modified ZIF-8-GA-CCM, and modified ZIF-8-GA-CCM-FA on different cell lines at 24 h (A) Hela, (B) A549, and (C) normal fibroblast cell lines.

https://doi.org/10.1021/acsomega.2c06705
ACS Omega 2023, 8, 3245−3257

good pH-responsive drug delivery vehicle; however, due to the general small pore size of nanoporous ZIF-8, in situ CCM encapsulation during the ZIF-8 synthesis process can be better compared to the postsynthesis drug loading method. The one-pot encapsulation of CCM in the ZIF-8-GA synthetic medium resulted in the high loading of CCM with DLE% and DLC% of 90 and 3.3%, respectively.

The investigation of the cytotoxicity of ZIF-8-GA, ZIF-8-GA-CCM, and ZIF-8-GA-CCM-FA structures by MTT assay on the three cell lines (Fibroblast (normal cell), Hela (FR-positive), and A549 (FR-negative) showed that the modified ZIF-8-GA-CCM-FA framework can have a promising effect on the targeted treatment of cancer Hela cells with an SI value of 2.7.

■ ASSOCIATED CONTENT

Supporting Information

The Supporting Information is available free of charge at https://pubs.acs.org/doi/10.1021/acsomega.2c06705.

The SEM image and size distribution histogram of ZIF-8, calibration curve of CCM, the in vitro releasing profile of CCM based on ppm, MTT assay analysis of different samples, and values of IC_{50} for different samples (PDF)

■ AUTHOR INFORMATION

Corresponding Author

Maryam Tohidi − *Department of Nanochemical Engineering, Faculty of Advanced Technologies, Shiraz University, Shiraz 71946-84636, Iran;* orcid.org/0000-0001-7907-2012; Email: matohidi@Shirazu.ac.ir

Authors

Seyedeh Fatemeh Khalilian − *Department of Nanochemical Engineering, Faculty of Advanced Technologies, Shiraz University, Shiraz 71946-84636, Iran*

Banafsheh Rastegari − *Diagnostic Laboratory Sciences and Technology Research Center, School of Paramedical Sciences, Shiraz University of Medical Sciences, Shiraz 7143918596, Iran*

Complete contact information is available at: https://pubs.acs.org/10.1021/acsomega.2c06705

Notes

The authors declare no competing financial interest.

■ ACKNOWLEDGMENTS

This research was supported by Shiraz University and Iran ministry of science and technology. The authors wish to thank all who assisted in conducting this work.

■ REFERENCES

(1) Tiwari, A.; Singh, A.; Garg, N.; Randhawa, J. K. Curcumin encapsulated zeolitic imidazolate frameworks as stimuli responsive drug delivery system and their interaction with biomimetic environment. *Sci. Rep.* **2017**, *7*, 12598.

(2) Mura, S.; Nicolas, J.; Couvreur, P. Stimuli-responsive nanocarriers for drug delivery. *Nat. Mater.* **2013**, *12*, 991−1003.

(3) Li, Y.; He, H.; Lu, W.; Jia, X. A poly (amidoamine) dendrimer-based drug carrier for delivering DOX to gliomas cells. *RSC Adv.* **2017**, *7*, 15475−15481.

(4) Anwekar, H.; Patel, S.; Singhai, A. Liposome-as drug carriers. *Int. J. Pharm. Life Sci.* **2011**, *2*, 945−951.

(5) Furukawa, H.; Cordova, K. E.; O'Keeffe, M.; Yaghi, O. M. The chemistry and applications of metal-organic frameworks. *Science* **2013**, *341*, No. 1230444.

(6) Zhang, M.; Qin, X.; Xu, W.; Wang, Y.; Song, Y.; Garg, S.; Luan, Y. Engineering of a dual-modal phototherapeutic nanoplatform for single NIR laser-triggered tumor therapy. *J. Colloid Interface Sci.* **2021**, *594*, 493−501.

(7) Gao, W.; Chan, J. M.; Farokhzad, O. C. pH-responsive nanoparticles for drug delivery. *Mol. Pharmaceutics* **2010**, *7*, 1913−1920.

(8) Zhang, M.; Qin, X.; Zhao, Z.; Du, Q.; Li, Q.; Jiang, Y.; Luan, Y. A self-amplifying nanodrug to manipulate the Janus-faced nature of ferroptosis for tumor therapy. *Nanoscale Horiz.* **2022**, *7*, 198−210.

(9) Ren, X.; Wang, N.; Zhou, Y.; Song, A.; Jin, G.; Li, Z.; Luan, Y. An injectable hydrogel using an immunomodulating gelator for amplified tumor immunotherapy by blocking the arginase pathway. *Acta Biomater.* **2021**, *124*, 179−190.

(10) Long, J. R.; Yaghi, O. M. The pervasive chemistry of metal−organic frameworks. *Chem. Soc. Rev.* **2009**, *38*, 1213−1214.

(11) Horcajada, P.; Chalati, T.; Serre, C.; Gillet, B.; Sebrie, C.; Baati, T.; Eubank, J. F.; Heurtaux, D.; Clayette, P.; Kreuz, C.; Chang, J. S.; Hwang, Y. K.; Marsaud, V.; Bories, P. N.; Cynober, L.; Gil, S.; Férey, G.; Couvreur, P.; Gref, R. Porous metal−organic-framework nanoscale carriers as a potential platform for drug delivery and imaging. *Nat. Mater.* **2010**, *9*, 172−178.

(12) Forgan, R. S. Metal-organic frameworks: edible frameworks. *Encyclopedia of Inorganic and Bioinorganic Chemistry*; John Wiley & Sons, Ltd, 2011, 1 −13.

(13) Ren, H.; Zhang, L.; An, J.; Wang, T.; Li, L.; Si, X.; He, L.; Wu, X.; Wang, C.; Su, Z. Polyacrylic acid@ zeolitic imidazolate framework-8 nanoparticles with ultrahigh drug loading capability for pH-sensitive drug release. *Chem. Commun.* **2014**, *50*, 1000−1002.

(14) Keskin, S.; Kızılel, S. Biomedical applications of metal organic frameworks. *Ind. Eng. Chem. Res.* **2011**, *50*, 1799−1812.

(15) Hoop, M.; Walde, C.; Ricco, R.; Mushtaq, F.; Terzopoulou, A.; Chen, X.-Z.; DeMello, A. J.; Doonan, C. J.; Falcaro, P.; Nelson, B. J. Biocompatibility characteristics of the metal organic framework ZIF-8 for therapeutical applications. *Appl. Mater. Today* **2018**, *11*, 13−21.

(16) Khalilian, S. F.; Tohidi, M.; Rastegari, B. Synthesis of a biocompatible nanoporous zeolitic imidazolate framework-8 in the presence of Gum Arabic inspired by the biomineralization process. *CrystEngComm* **2020**, *22*, 1875−1884.

(17) Liang, K.; Wang, R.; Boutter, M.; Doherty, C. M.; Mulet, X.; Richardson, J. J. Biomimetic mineralization of metal−organic frameworks around polysaccharides. *Chem. Commun.* **2017**, *53*, 1249−1252.

(18) Wu, X.; Yang, C.; Ge, J. Green synthesis of enzyme/metal-organic framework composites with high stability in protein denaturing solvents. *Bioresour. Bioprocess.* **2017**, *4*, 24.

(19) Zhang, Q.; Li, Z.; Dai, H.; Zhang, L.; Zhang, J.; Liu, Y.; Lin, J.; Liang, K.; Ying, Y.; Li, Y.; Fu, Y. Biomineralization-mimetic growth of ultrahigh-load metal-organic frameworks on inert glass fibers to prepare hybrid membranes for collecting organic hazards in unconventional environment. *Chem. Eng. J.* **2022**, *430*, No. 132956.

(20) Xu, S.; Liang, J.; Mohammad, M. I. B.; Lv, D.; Cao, Y.; Qi, J.; Liang, K.; Ma, J. Biocatalytic metal−organic framework membrane towards efficient aquatic micropollutants removal. *Chem. Eng. J.* **2021**, *426*, No. 131861.

(21) Yan, S.; Zeng, X.; Wang, Y.; Liu, B. F. Biomineralization of bacteria by a metal−organic framework for therapeutic delivery. *Adv. Healthcare Mater.* **2020**, *9*, No. 2000046.

(22) Patel, S.; Goyal, A. Applications of natural polymer gum arabic: a review. *Int. J. Food Prop.* **2015**, *18*, 986−998.

(23) Sarika, P. R.; James, N. R.; Kumar, P. R. A.; Raj, D. K.; Kumary, T. V. Gum arabic-curcumin conjugate micelles with enhanced loading for curcumin delivery to hepatocarcinoma cells. *Carbohydr. Polym.* **2015**, *134*, 167−174.

(24) Priyadarsini, K. I. The chemistry of curcumin: from extraction to therapeutic agent. *Molecules* **2014**, *19*, 20091−20112.

(25) Anand, P.; Kunnumakkara, A. B.; Newman, R. A.; Aggarwal, B. B. Bioavailability of curcumin: problems and promises. *Mol. Pharmaceutics* **2007**, *4*, 807−818.
(26) Pillai, N. G.; Archana, K.; Rhee, K. Y.; Park, S.-J.; Asif, A. In vitro antiproliferative study of curcumin loaded nano zeolitic imidazolate framework hybrid biomaterials on HeLa cells. *J. Ind. Eng. Chem.* **2019**, *79*, 288−294.
(27) Liu, Z.; Wu, Q.; He, J.; Vriesekoop, F.; Liang, H. Crystal-seeded growth of pH-responsive metal−organic frameworks for enhancing encapsulation, stability, and bioactivity of hydrophobicity compounds. *ACS Biomater. Sci. Eng.* **2019**, *5*, 6581−6589.
(28) Moussa, Z.; Hmadeh, M.; Abiad, M. G.; Dib, O. H.; Patra, D. Encapsulation of curcumin in cyclodextrin-metal organic frameworks: Dissociation of loaded CD-MOFs enhances stability of curcumin. *Food Chem.* **2016**, *212*, 485−494.
(29) Karimi Alavijeh, R.; Akhbari, K. Biocompatible MIL-101 (Fe) as a smart carrier with high loading potential and sustained release of curcumin. *Inorg. Chem.* **2020**, *59*, 3570−3578.
(30) Gao, X.; Hai, X.; Baigude, H.; Guan, W.; Liu, Z. Fabrication of functional hollow microspheres constructed from MOF shells: Promising drug delivery systems with high loading capacity and targeted transport. *Sci. Rep.* **2016**, *6*, 37705.
(31) Laha, D.; Pal, K.; Chowdhuri, A. R.; Parida, P. K.; Sahu, S. K.; Jana, K.; Karmakar, P. Fabrication of curcumin-loaded folic acid-tagged metal organic framework for triple negative breast cancer therapy in in vitro and in vivo systems. *New J. Chem.* **2019**, *43*, 217−229.
(32) Chowdhuri, A. R.; Laha, D.; Pal, S.; Karmakar, P.; Sahu, S. K. One-pot synthesis of folic acid encapsulated upconversion nanoscale metal organic frameworks for targeting, imaging and pH responsive drug release. *Dalton Trans.* **2016**, *45*, 18120−18132.
(33) Li, J.; Shin, G. H.; Lee, I. W.; Chen, X.; Park, H. J. Soluble starch formulated nanocomposite increases water solubility and stability of curcumin. *Food Hydrocolloids* **2016**, *56*, 41−49.
(34) Hudiyanti, D.; Al Khafiz, M. F.; Anam, K.; Siahaan, P.; Christa, S. M. In vitro evaluation of curcumin encapsulation in gum arabic dispersions under different environments. *Molecules* **2022**, *27*, 3855.
(35) Sareen, R.; Jain, N.; Dhar, K. L. Curcumin−Zn (II) complex for enhanced solubility and stability: an approach for improved delivery and pharmacodynamic effects. *Pharm. Dev. Technol.* **2016**, *21*, 630−635.
(36) Jian, M.; Liu, B.; Liu, R.; Qu, J.; Wang, H.; Zhang, X. Water-based synthesis of zeolitic imidazolate framework-8 with high morphology level at room temperature. *RSC Adv.* **2015**, *5*, 48433−48441.
(37) Pan, Y.; Heryadi, D.; Zhou, F.; Zhao, L.; Lestari, G.; Su, H.; Lai, Z. Tuning the crystal morphology and size of zeolitic imidazolate framework-8 in aqueous solution by surfactants. *CrystEngComm* **2011**, *13*, 6937−6940.
(38) Wang, Z.; Ren, D.; Yu, H.; Jiang, S.; Cheng, Y.; Zhang, S.; Zhang, X. Adsorption kinetic and isothermal studies of 2, 4-dichlorophenol from aqueous solutions with zeolitic imidazolate framework-8 (ZIF-8). *Environ. Eng. Sci.* **2021**, *38*, 537−546.
(39) Zheng, H.; Zhang, Y.; Liu, L.; Wan, W.; Guo, P.; Nyström, A. M.; Zou, X. One-pot synthesis of metal−organic frameworks with encapsulated target molecules and their applications for controlled drug delivery. *J. Am. Chem. Soc.* **2016**, *138*, 962−968.
(40) Wang, Q.; Sun, Y.; Li, S.; Zhang, P.; Yao, Q. Synthesis and modification of ZIF-8 and its application in drug delivery and tumor therapy. *RSC Adv.* **2020**, *10*, 37600−37620.
(41) Bashir, M.; Haripriya, S. Assessment of physical and structural characteristics of almond gum. *Int. J. Biol. Macromol.* **2016**, *93*, 476−482.
(42) Feng, R.; Song, Z.; Zhai, G. Preparation and in vivo pharmacokinetics of curcumin-loaded PCL-PEG-PCL triblock co-polymeric nanoparticles. *Int. J. Nanomed.* **2012**, *7*, 4089−4098.
(43) Rana, S.; Shetake, N. G.; Barick, K. C.; Pandey, B. N.; Salunke, H. G.; Hassan, P. A. Folic acid conjugated Fe 3 O 4 magnetic nanoparticles for targeted delivery of doxorubicin. *Dalton Trans.* **2016**, *45*, 17401−17408.
(44) Taylor-Pashow, K. M. L.; Della Rocca, J.; Xie, Z.; Tran, S.; Lin, W. Postsynthetic modifications of iron-carboxylate nanoscale metal−organic frameworks for imaging and drug delivery. *J. Am. Chem. Soc.* **2009**, *131*, 14261−14263.
(45) Soltani, B.; Nabipour, H.; Nasab, N. A. Efficient storage of gentamicin in nanoscale zeolitic imidazolate framework-8 nanocarrier for pH-responsive drug release. *J. Inorg. Organomet. Polym. Mater.* **2018**, *28*, 1090−1097.
(46) Wang, X.-G.; Dong, Z.-Y.; Cheng, H.; Wan, S.-S.; Chen, W.-H.; Zou, M.-Z.; Huo, J.-W.; Deng, H.-X.; Zhang, X.-Z. A multifunctional metal−organic framework based tumor targeting drug delivery system for cancer therapy. *Nanoscale* **2015**, *7*, 16061−16070.
(47) Maranescu, B.; Visa, A. Applications of Metal-Organic Frameworks as Drug Delivery Systems. *Int. J. Mol. Sci.* **2022**, *23*, 4458.
(48) Easton, D. F.; Pooley, K. A.; Dunning, A. M.; Pharoah, P. D.; Thompson, D.; Ballinger, D. G.; Struewing, J. P.; Morrison, J.; Field, H.; Luben, R.; Wareham, N.; Ahmed, S.; Healey, C. S.; Bowman, R.; The SEARCH collaborators; Luccarini, C.; Conroy, D.; Shah, M.; Munday, H.; Jordan, C.; Perkins, B.; West, J.; Redman, K.; Driver, K.; Meyer, K. B.; Haiman, C. A.; Kolonel, L. K.; Henderson, B. E.; le Marchand, L.; Brennan, P.; Sangrajrang, S.; Gaborieau, V.; Odefrey, F.; Shen, C. Y.; Wu, P. E.; Wang, H. C.; Eccles, D.; Evans, D. G.; Peto, J.; Fletcher, O.; Johnson, N.; Seal, S.; Stratton, M. R.; Rahman, N.; Chenevix-Trench, G.; Bojesen, S. E.; Nordestgaard, B. G.; Axelsson, C. K.; Garcia-Closas, M.; Brinton, L.; Chanock, S.; Lissowska, J.; Peplonska, B.; Nevanlinna, H.; Fagerholm, R.; Eerola, H.; Kang, D.; Yoo, K. Y.; Noh, D. Y.; Ahn, S. H.; Hunter, D. J.; Hankinson, S. E.; Cox, D. G.; Hall, P.; Wedren, S.; Liu, J.; Low, Y. L.; Bogdanova, N.; Schürmann, P.; Dörk, T.; Tollenaar, R. A. E. M.; Jacobi, C. E.; Devilee, P.; Klijn, J. G. M.; Sigurdson, A. J.; Doody, M. M.; Alexander, B. H.; Zhang, J.; Cox, A.; Brock, I. W.; MacPherson, G.; Reed, M. W. R.; Couch, F. J.; Goode, E. L.; Olson, J. E.; Meijers-Heijboer, H.; van den Ouweland, A.; Uitterlinden, A.; Rivadeneira, F.; Milne, R. L.; Ribas, G.; Gonzalez-Neira, A.; Benitez, J.; Hopper, J. L.; McCredie, M.; Southey, M.; Giles, G. G.; Schroen, C.; Justenhoven, C.; Brauch, H.; Hamann, U.; Ko, Y. D.; Spurdle, A. B.; Beesley, J.; Chen, X.; kConFab; Aghmesheh, M.; Amor, D.; Andrews, L.; Antill, Y.; Armes, J.; Armitage, S.; Arnold, L.; Balleine, R.; Begley, G.; Beilby, J.; Bennett, I.; Bennett, B.; Berry, G.; Blackburn, A.; Brennan, M.; Brown, M.; Buckley, M.; Burke, J.; Butow, P.; Byron, K.; Callen, D.; Campbell, I.; Chenevix-Trench, G.; Clarke, C.; Colley, A.; Cotton, D.; Cui, J.; Culling, B.; Cummings, M.; Dawson, S. J.; Dixon, J.; Dobrovic, A.; Dudding, T.; Edkins, T.; Eisenbruch, M.; Farshid, G.; Fawcett, S.; Field, M.; Firgaira, F.; Fleming, J.; Forbes, J.; Friedlander, M.; Gaff, C.; Gardner, M.; Gattas, M.; George, P.; Giles, G.; Gill, G.; Goldblatt, J.; Greening, S.; Grist, S.; Haan, E.; Harris, M.; Hart, S.; Hayward, N.; Hopper, J.; Humphrey, E.; Jenkins, M.; Jones, A.; Kefford, R.; Kirk, J.; Kollias, J.; Kovalenko, S.; Lakhani, S.; Leary, J.; Lim, J.; Lindeman, G.; Lipton, L.; Lobb, L.; Maclurcan, M.; Mann, G.; Marsh, D.; McCredie, M.; McKay, M.; Anne McLachlan, S.; Meiser, B.; Milne, R.; Mitchell, G.; Newman, B.; O'Loughlin, I.; Osborne, R.; Peters, L.; Phillips, K.; Price, M.; Reeve, J.; Reeve, T.; Richards, R.; Rinehart, G.; Robinson, B.; Rudzki, B.; Salisbury, E.; Sambrook, J.; Saunders, C.; Scott, C.; Scott, E.; Scott, R.; Seshadri, R.; Shelling, A.; Southey, M.; Spurdle, A.; Suthers, G.; Taylor, D.; Tennant, C.; Thorne, H.; Townshend, S.; Tucker, K.; Tyler, J.; Venter, D.; Visvader, J.; Walpole, I.; Ward, R.; Waring, P.; Warner, B.; Warren, G.; Watson, E.; Williams, R.; Wilson, J.; Winship, I.; Young, M. A.; AOCS Management Group; Bowtell, D.; Green, A.; deFazio, A.; Chenevix-Trench, G.; Gertig, D.; Webb, P.; Mannermaa, A.; Kosma, V. M.; Kataja, V.; Hartikainen, J.; Day, N. E.; Cox, D. R.; Ponder, B. A. J. Genome-wide association study identifies novel breast cancer susceptibility loci. *Nature* **2007**, *447*, 1087−1093.
(49) Clark, A. G.; Eisen, M. B.; Smith, D. R.; Bergman, C. M.; Oliver, B.; Markow, T. A.; Kaufman, T. C.; Kellis, M.; Gelbart, W.; Iyer, V. N. Evolution of genes and genomes on the Drosophila phylogeny. *Nature* **2007**, *450*, 203−218.

https://doi.org/10.1021/acsomega.2c06705
ACS Omega 2023, 8, 3245−3257

(50) Low, N.; Butt, S.; Ellis, P.; Davis Smith, J., *Helping out: A national survey of volunteering and charitable giving*. 2007.
(51) Ranjitkar, S.; Zhang, D.; Sun, F.; Salman, S.; He, W.; Venkitanarayanan, K.; Tulman, E. R.; Tian, X. Cytotoxic effects on cancerous and non-cancerous cells of trans-cinnamaldehyde, carvacrol, and eugenol. *Sci. Rep.* **2021**, *11*, 16281.

https://doi.org/10.1021/acsomega.2c06705
ACS Omega 2023, 8, 3245−3257